Title

Intercellular signaling stabilizes single-cell level phenotypic transitions and accelerates the reestablishment of equilibrium of heterogeneous cancer cell populations

Author list

Daniel Lopez [1], Darren R Tyson [2], Tian Hong [3*]

Affiliation

[1] Department of Biochemistry & Cellular and Molecular Biology, The University of Tennessee, Knoxville. Knoxville, Tennessee 37916, USA

[2] Department of Pharmacology and Cancer Biology, Duke University School of Medicine, Durham, North Carolina 27710, USA

[3] Department of Biological Sciences, The University of Texas at Dallas. Richardson, Texas 75080, USA

[*] To whom correspondence should be addressed to

E-mail: hong@utdallas.edu

Abstract

Cancer cells within tumors exhibit a wide range of phenotypic states driven by non-genetic mechanisms in addition to extensively studied genetic alterations. Conversions among cancer cell states can result in intratumoral heterogeneity which contributes to metastasis and development of drug resistance. However, mechanisms underlying the initiation and/or maintenance of such phenotypic plasticity are poorly understood. In particular, the role of intercellular communications in phenotypic plasticity remains elusive. In this study, we employ a multiscale inference-based approach using single-cell RNA sequencing (scRNA-seq) data to explore how intercellular interactions influence phenotypic dynamics of cancer cells, particularly cancers undergoing epithelial-mesenchymal transition. Our inference approach reveals that signaling interactions between cancerous cells in small cell lung cancer (SCLC) result in seemingly contradictory behaviors—reinforcing the cellular phenotypes and maintaining population-level intratumoral heterogeneity. Additionally, we find a recurring signaling pattern across multiple types of cancer in which the mesenchymal-like subtypes utilize signals from other subtypes to reinforce its phenotype, further promoting the intratumoral heterogeneity. We use a mathematical model based on ordinary differential equations to show that inter-subtype communication accelerates the development of heterogeneous tumor populations. Our work highlights the critical role of intercellular signaling in sustaining intratumoral heterogeneity, and our approach of computational analysis of scRNA-seq data can infer inter- and intra-cellular signaling networks in a holistic manner.

Significance

Single cell-based inference approach reveals a key role of intercellular signaling in maintaining intratumoral heterogeneity. Cell-cell communications stabilize newly acquired cell states and diverse phenotypes of cell populations in multiple cancers.

Introduction

Most tumors develop and evolve as complex ecosystems under strong environmental selective pressures, leading to a unique collection of cancer cells that exhibit a wide range of genotypic and phenotypic characteristics[1,2]. This intratumoral heterogeneity promotes aggressive disease progression, increased resistance to therapeutic interventions, and poor overall survival[1,3–5]. While genetic diversity is a well-known driver of intratumoral heterogeneity[6], there is increasing evidence that non-genetic mechanisms, such as epigenetic, transcriptional, and/or translational changes, also significantly contribute to the intratumoral heterogeneity and disease progression[4,5,7,8]. These non-genetic mechanisms can create distinct cancer cell states through a process called phenotypic plasticity, where cells are dynamic, reversible, and responsive to regulatory changes[3,9,10].

Phenotypic plasticity has recently been recognized as a hallmark of cancer and a key driver of tumor aggressiveness[3]. It influences various cellular behaviors in cancer,

including stemness and differentiation, drug-sensitive and drug-resistant states, and transitions between epithelial and mesenchymal cell-states[11]. Increasing efforts are being made to characterize the intrinsic cellular factors that drive phenotypic plasticity[12–14]. However, despite extensive molecular characterization, the dynamics of phenotypic plasticity at the single-cell and population levels remain largely unclear. This is particularly true regarding how non-cell-autonomous effects regulate intratumoral heterogeneity and whether the intercellular communication between different cell states stabilizes or destabilizes these phenotypes.

One such cancer where phenotypic plasticity is particularly evident is small cell lung cancer (SCLC)[15,16]. SCLC is a neuroendocrine (NE) carcinoma that constitutes approximately 15 percent of all lung cancer cases and has a dismal 5-year survival rate of less than 7 percent[17]. Despite the high similarity to pulmonary NE cells and having highly consistent morphological characteristics, SCLC presents substantial inter- and intratumoral heterogeneity, featuring distinct molecular subtypes with varied biological behaviors[18–22]. These subtypes are categorized based on the enriched expression of one of four transcription factors (TFs): *ASCL1*, *NEUROD1*, *POU2F3*, *YAP1*[23]. Furthermore, these subtypes delineate into two overarching categories, NE (A2, A, and N) and non-NE (P and Y), with the NE subtypes typically exhibiting some level of ASCL1 expression while non-NE counterparts do not. Recent studies have demonstrated that SCLC tumors will often comprise multiple cell types, with the different subtypes cooperating to drive tumorgenicity[21,22]. The dynamic regulation of TFs regulates intratumoral compositions, and this diversity is essential as different subtypes play distinct biological roles, impacting therapeutic response[21,22].

Further highlighting the phenotypic plasticity evident within SCLC, previous work by us[24] and others[25,26] has linked the different SCLC subtypes to the epithelial-mesenchymal transition (EMT) program, a cellular process in which cell-cell interactions are remodeled, resulting in cells losing their epithelial properties and assuming a more mesenchymal phenotype.[27]. Within SCLC, the NE subtype A2 demonstrates a strong epithelial-like phenotype whereas the other NE subtypes, A and N, display a partial EMT state (Figure 1A). Non-NE subtypes, P and Y, also display a partial EMT state, albeit with mesenchymal gene expression signatures that differ from that of the NE subtypes. This correspondence with EMT further demonstrates the plastic nature of this cancer.

Most research on SCLC has focused on describing its differing cell states, with very few studies attempting to define these states at the single-cell level. Consequently, there is still much to learn about the transitions between different cell states and whether intercellular communication influences the intratumoral heterogeneity. Given the plasticity present within SCLC, we utilized single-cell RNA-sequencing (scRNA-seq) SCLC data to investigate whether intercellular communications influence cell-fate transitions, and if so, whether these extracellular signals reinforce the current phenotype of a cell or push it towards a different phenotype.

To investigate whether intercellular communications play a role in driving intratumoral heterogeneity within SCLC, we adapted a single-cell multiscale inference-based approach that integrates both intercellular interactions and intracellular signaling dynamics. By linking inter- and intracellular signaling, we aim to determine if intercellular interactions impact downstream intracellular mechanisms. If cell–cell communication affects downstream signaling, this approach will also reveal whether these interactions drive the cell towards a different phenotype or reinforce its current one (Figure 1B). To explore the effect of cell–cell communications on phenotypic heterogeneity, we utilized scRNA-seq data from ex vivo cultured cells obtained from a genetically engineered mouse model that incorporates a constitutively active form of *MYC*, coincident with deletions of *Rb* and *p53* (RPM)[28]. The cells undergo a transition over time in culture from a NE to non-NE state and these time series data enable the exploration of intercellular communications between the NE and Non-NE populations at individual time points. Through this approach, we identified the activation of several well-established EMT pathways, revealing a consistent pattern of convergence towards activating mesenchymal genes within the mesenchymal phenotype. Additionally, our analysis revealed that the epithelial phenotype employs both paracrine and autocrine signaling mechanisms to maintain its epithelial state. To see if these mechanisms are consistent across epithelial cancers that involve EMT, we applied this method to colon and breast cancer datasets. The convergence of EMT pathways towards the mesenchymal phenotype is present across all 3 cancers. However, SCLC appears to be unique in its utilization of both paracrine and autocrine signals to sustain its phenotypic state. Overall, our results show recurring roles of intercellular communications in maintaining newly formed cell states, and they shed light into non-cell-autonomous mechanisms of intratumoral heterogeneity.

A multiscale inference approach to explore the signaling mechanisms maintaining phenotypic heterogeneity in cancer cell populations

To assess whether cell-cell communications contribute to intratumoral heterogeneity and phenotypic plasticity it is essential to connect intercellular signaling with downstream intracellular processes and determine their overall impact on maintaining phenotypic diversity. To link intercellular communication with intracellular signaling, we adapted the LIANA+[29] methodology (see Methods) (Figure 1C), which integrates various approaches to explore both intercellular and intracellular signaling events. Briefly, we used *CellChat*[30] to infer the intercellular communications from processed scRNA-seq data. We opted for *CellChat* over alternative cell-cell communication inference methods due to its capacity to incorporate heteromeric complexes and its robustness to noise[31]. *CellChat* infers active signaling pathways and ligand–receptor (L–R) interactions, which are subsequently used to assess intracellular signaling.

The active signaling pathways inferred by CellChat are used to predict transcriptional activity and identify the relative strength of active signaling pathways in each cell state. We used *CARNIVAL*[32], an integer linear programming based tool for contextualizing causal networks, to integrate the transcription factor (TF) activity inference scores, differential expression analysis and L-R interactions. This algorithm will find the smallest-sign consistent network that explains the measured inputs and outputs, connecting the receptors to the downstream TFs. To aid in assessing the relationships between EMT states cellular differentiation, we incorporate downstream EMT target genes in the network—adding EMT-specific genes based on the congruence between regulatory modes (i.e. activation or inhibition) and gene expression. This multiscale integration allows us to capture dynamic changes in signaling networks across different cell states and enables a detailed exploration of the potential signaling mechanisms involved in maintaining the phenotypic heterogeneity within the cancerous population.

We applied this approach to the SCLC RPM dataset, focusing primarily on timepoints 7 and 11, when both NE and non-NE subtypes are present in relatively high abundance (Figure 1D). Within this dataset, five subtypes were determined via archetype analysis (A2, A/N, P/Y, Y and None), with the A2 subtype displaying more epithelial-like properties, while the P/Y and Y subtypes exhibited more mesenchymal like features, as expected. We then extended this approach to three additional datasets involving cancers undergoing EMT: SC53 (Human SCLC circulating tumor cells-derived xenograft sample[25]), HCT116 colon cancer cell line[33], and a HER2 Crainbow mouse[34](Figure 1E & Supplementary Figure 1). The cell type classifications in these datasets were determined by the authors who generated the data. In SC53 there are four identified subtypes: A, A2, Y and Generalists, which is a non-specified cell type from archetype analysis. Notably, the Y subtype exhibited gene expression profiles consistent with a more mesenchymal-like state. In the colon cancer dataset, three EMT-associated states were characterized: epithelial (Epi), mesenchymal (Mes), and partial-EMT (pEMT). The HER2 dataset has four cell-states that were inferred through trajectory analysis: hormone-sensitive (HS), hormone-receptor negative (HS-), EMT and a transitional (T) state.

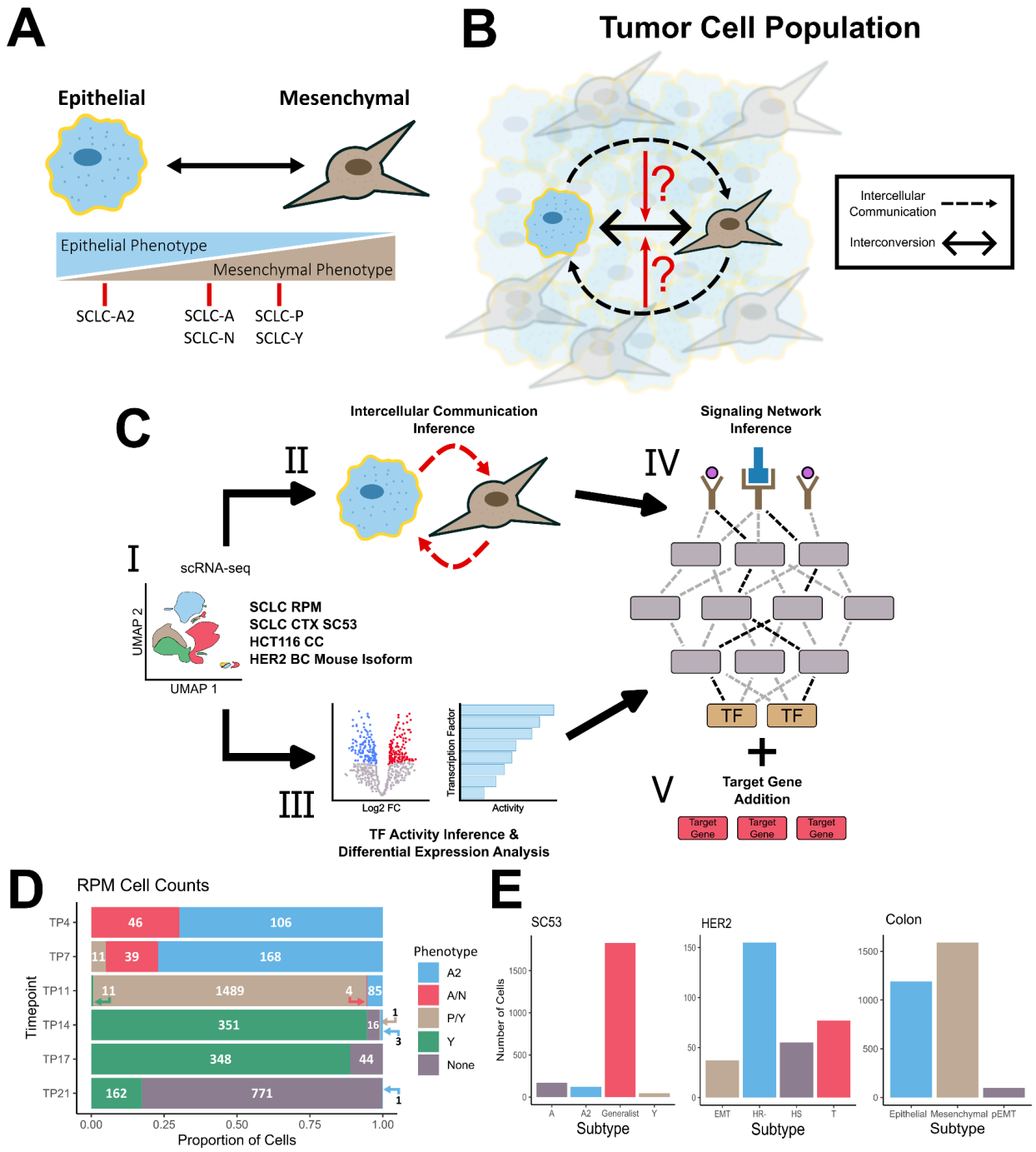

Figure 1: ***Multiscale Inference Approach to Investigate Role of Intercellular Communication on Cellular Plasticity.*** *A) Schematic depicting EMT and correspondence to SCLC subtypes. Subtypes are characterized based on transcriptomic expression. B) Investigating whether intercellular communications affect the cell state transitions between subtypes and the overall intratumoral heterogeneity. Black dashed arrows represent inferred cell-cell communication and the black, double-arrow represents the interconversion between subtypes. C) I: Pre-processed and annotated scRNA-seq data. Pipeline is applied to four different datasets across three different cancers II: Inference of cell-cell communications using CellChat. III: Differential expression and transcription factor activity analysis. IV: Signaling network inference via CORNETO is*

performed using the receptor probability and transcription factor activity scores as inputs. v: Differentially expressed SCLC and EMT gene markers are added to the network based on filtering criteria. D) Filled bar chart showing the cell counts for the RPM dataset. X-axis represents the proportion of cells and y-axis is the time point. The cell numbers for each cell type are shown. E) Cell counts for SCLC SC53, HER2 and colon cancer datasets, respectively.

Diverse signaling pathways converge on activating key mesenchymal pathways/genes

We first analyzed the RPM dataset and identified 48 active signaling pathways across the six different timepoints (Supplementary Table 1). Many of these pathways are well-established contributors to EMT in cancer[27,35–56] (Figure 2A). Notably, we observed a recurring pattern among these EMT pathways wherein they converge towards the mesenchymal non-NE cell types (P/Y in Figure 2B). This convergence is mediated by paracrine (NOTCH) signaling from NE to non-NE cells and autocrine signaling within the non-NE cell population (WNT and SPP1).

To elucidate how the intercellular communication affects intracellular signaling, we constructed a signaling network for the Day 7 P/Y cell type that has TGFβ and NOTCH as primary ligands and captured key lineage-supporting target genes (Figure 2C). Within the network, we observed the activation of numerous mesenchymal markers (like vimentin, PDGF-C and Axl) and the inhibition of epithelial markers, especially Epcam. Consistent with previous experimental findings[16], we noted that the activation of *Myc* and Notch signaling promotes the non-NE SCLC fate. Our network further highlights that the inhibition of *Ascl1*—a NE and SCLC-A & -A2 subtype marker downstream of the *Notch2* receptor—and the activation of *Myc* facilitates the upregulation of mesenchymal markers. Notably, the ligand–receptor interactions captured in the network are well known EMT modulators. Since the ligands involved in the activation of mesenchymal markers within the P/Y network originate from A2, A/N and P/Y cells, our network underscores the contributions of both NE and non-NE cells toward mesenchymal transitions.This approach yielded similar results in the Day 11 P/Y cell type by capturing the activation of lineage-supporting genes, with both NE and non-NE cells playing a role in activating those genes (Supplementary Figure 2). We assessed the importance of lineage supporting genes to the networks inferred from the differentially expressed genes downstream of the detected L–R pairs by determining the proportion of lineage supporting genes included in the inferred signaling networks versus excluded from the network. We found a higher proportion of lineage supporting genes within the network compared to outside the network (Figure 2D) (Supplementary Table 2), suggesting that the inferred intercellular communication driving the mesenchymal (M) state transcriptional program was not simply due to the random selection of broadly upregulated M genes.

To assess the generalizability of these findings across other cancers undergoing EMT, we performed a similar analysis on three additional scRNA-seq datasets. We observed the activation of intercellular communication-driven mesenchymal pathways converging towards a more mesenchymal phenotype in all three datasets (Figure 2E). However, application of the signaling network pipeline to the colon and HER2 datasets yielded less comprehensive networks compared to those observed in SCLC

(Supplementary Figure 3). This discrepancy suggests potential differences in the sensitivity to detect extracellular signals or a reduced influence of the tumor microenvironment in driving phenotypic heterogeneity within these datasets. Overall, our findings demonstrate that the intercellular communications between cancer cells can have varying degrees of influence in maintaining phenotypic diversity. Within SCLC, the intercellular communications between NE and non-NE phenotypes reinforce the non-NE/mesenchymal (P/Y or Y) state.

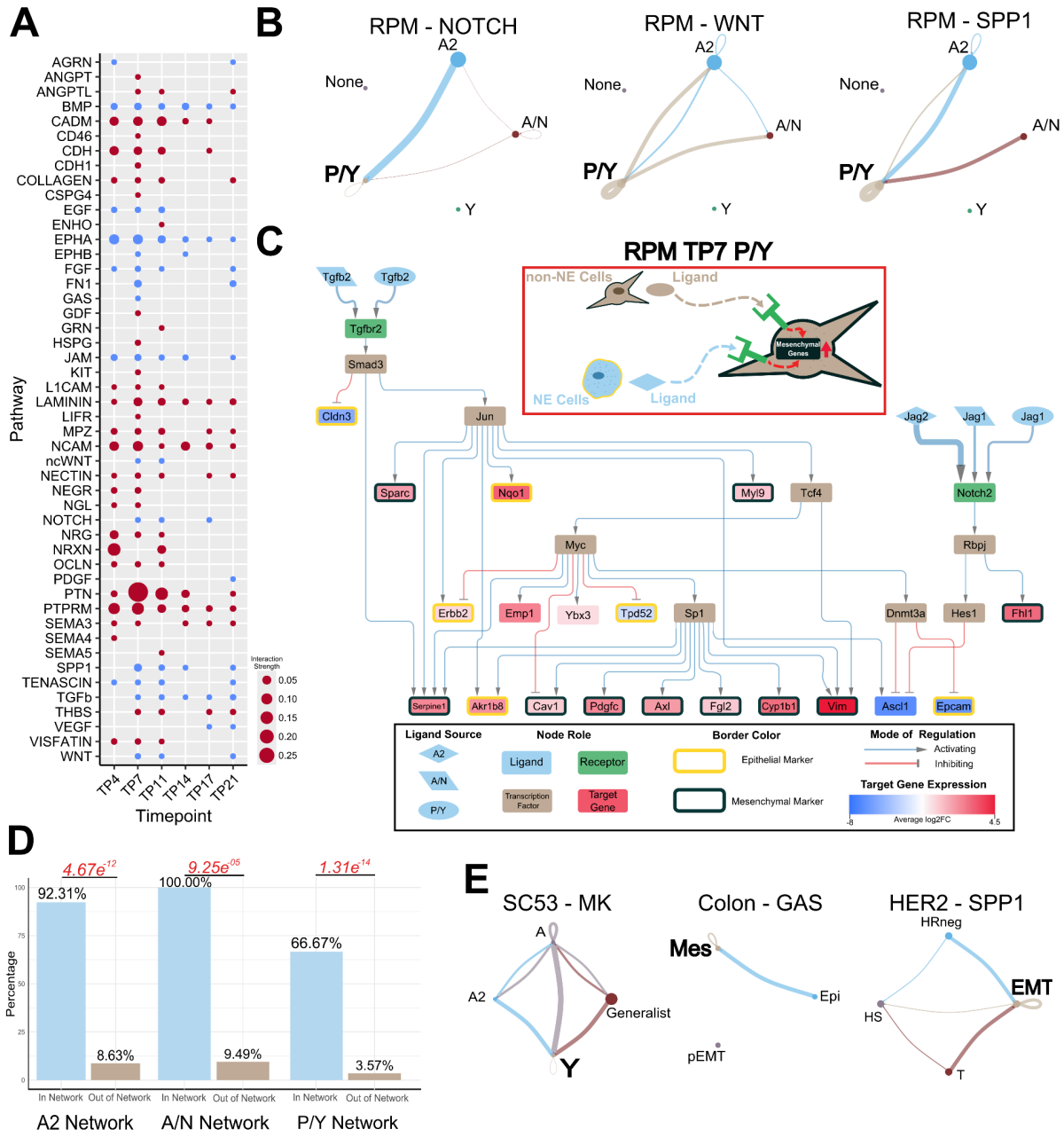

Figure 2: ***Mesenchymal Phenotypes Utilize Autocrine and Paracrine Signaling to Reinforce SCLC Subtypes.*** A) Inferred active pathways in the SCLC dataset. Dot size is representative of the relative interaction strength for a given time point. B) Inferred *CellChat* signaling of pathways known to be involved in EMT. Dot size is proportional to cell number. Line color

represents source of signal/ligand. Line width represents interaction strength. C) RPM TP7 P/Y cell type inferred signaling network connecting both intercellular and intracellular signaling. The red box contains an illustrative summary of the network. The black box is a legend for the network. Node fill color represents a role in signaling pathway. The shape of the ligand nodes represents the subtype source of the ligand. The edges connecting a ligand to receptor vary in width corresponding to interaction strength. Average log2 fold-change of target gene expression is colored as indicated by the scale bar. Epithelial target genes are indicated by a yellow border around the node and mesenchymal genes have a black border. D) Proportion of lineage supporting genes included in (In Network) and excluded from (Out of Network) the network. Fisher's exact test was used to calculate significance. P-values are labeled in red. Odds ratios from left to right: 126.99, inf, 54.08. E) Inferred *CellChat* signaling of EMT pathways from other datasets. Left: Human SCLC CDX. Subtypes are characterized through archetype analysis. Middle: HCT116 colon cancer. Subtype labels are Epi (Epithelial), Mes (Mesenchymal), and pEMT (Partial EMT) and they are from the original publication. Left: HER2 breast cancer mouse. Subtype labels are HS (Hormone-sensitive), HR-negative (Hormone-receptor negative), T (Transitional state), and EMT. The more mesenchymal states in these datasets are, Y, Mes, and EMT, respectively.

SCLC utilizes autocrine and paracrine signaling to maintain epithelial state

We next asked how the cross-talk between the different states affects the epithelial state. In the RPM dataset, our analysis revealed that the epithelial state is sustained through a combination of paracrine and autocrine signaling mechanisms. We applied our analytical pipeline to construct a network for the Day 7 epithelial, A2 subtype (Figure 3A). The network captured the activation of several epithelial marker genes. We observed the activation of the epithelial marker *Cdh1* in both the Day 7 and Day 11 network (Supplementary Figure 4). Additionally, the Day 7 network showed the activation of the A2 marker, *Ascl1*. Notably, we identified *Sp1* as a key transcription factor involved in the activation of several epithelial markers. Interestingly, *Sp1* was also present in the P/Y network, suggesting its potential to influence both NE and non-NE cell fate determination.

Similar to observations in the P/Y network, the A2 network revealed the participation of both NE and non-NE cells in maintaining the epithelial state within A2 cells. This interplay is also evident in the other inferred signaling pathways (Figure 3B). Specifically, the inferred interaction involving *Jam3* ligands within the JAM signaling pathway is consistent with prior work demonstrating *Jam3*'s role in establishing the epithelial phenotype[57]. Furthermore, we identified the CDH1 pathway as being activated by autocrine signaling within A2 cells. The presence of CDH1 and JAM signaling pathways was also observed in human SCLC SC53 samples, operating in a manner similar to our findings in the A2 network (Figure 3C and Supplementary Figure 5). This suggests that the maintenance of the SCLC epithelial state involves signaling interactions between epithelial and mesenchymal cells.

When applying the signaling network pipeline to the epithelial states of the other cancers, a network could only be generated for the colon cancer epithelial state but not the HER2 epithelial states (Supplementary Figure 3). The colon cancer network does not capture the activation of any of the overexpressed epithelial genes present within this cell type. For the HER2 epithelial states, a causal inference network could not be generated from the receptors to transcription factors. However, the less comprehensive nature of the colon cancer network and the inability to generate a network for the HER2 epithelial state could be due to additional mechanisms playing a role in either maintaining or destabilizing the epithelial state. This highlights the different levels of

influence that cell–cell communication may play in maintaining the intratumoral heterogeneity, with the epithelial SCLC state being more sensitive to these signals.

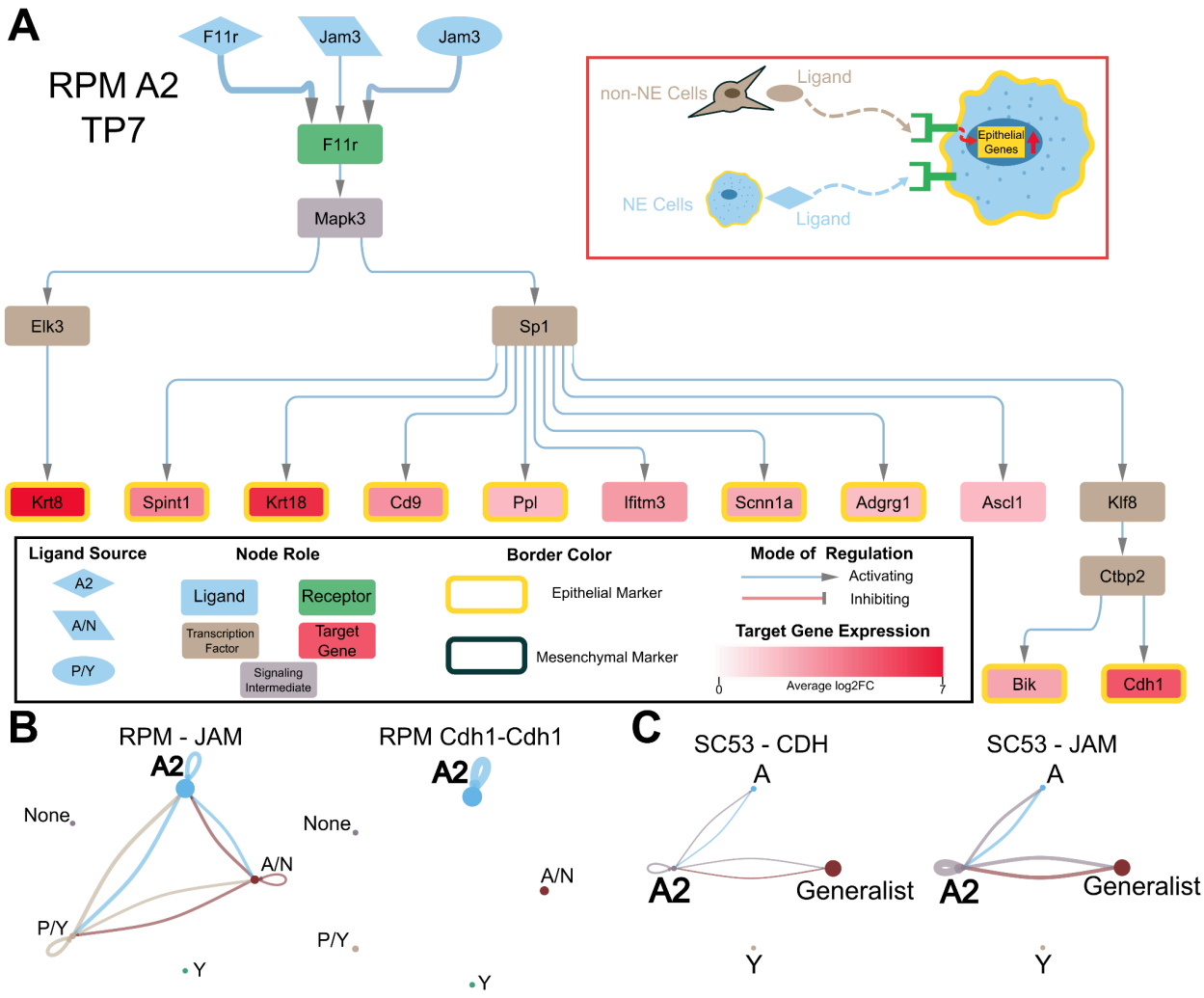

Figure 3: ***Epithelial Phenotype is Maintained by Autocrine and Paracrine Signaling.*** A) RPM TP7 A2 cell type inferred signaling network. The inset indicated with a red rectangle is an illustrative summary of the network. The legend of the network is shown in the inset black rectangle. B) From the RPM data, the inferred JAM signaling pathway is shown on the left and the inferred ligand-receptor interaction of CDH1 is shown on the right. C) Inferred CDH signaling pathway (left) and JAM pathway (right) from the human SCLC SC53 dataset.

A mathematical model predicts a role of inter-subtype feedback in restoring heterogeneous tumor cell population

Through our inference pipeline we found a pattern of intercellular communication shared by multiple cancer types and datasets: cells at the state enriched with mesenchymal (M) genes receive signals from cells at a more epithelial-like state, and the signals were used to maintain the recently acquired M state. While we found intra-subtype signals that also help to maintain the new state, the functions of these autocrine-like signals were well characterized in previous studies[58,59]. It was unclear, however, how the inter-subtype signals that we found in multiple contexts can influence intratumoral

population dynamics. We therefore built a simple mathematical model based on the following ordinary differential equations (ODEs)

$$dX_1/dt = r_1X_1 - k_1X_1 + 1/(1 + (w_1/K_2)^{n_2})k_2X_2 \quad (1)$$

$$dX_2/dt = r_2X_2 + k_1X_1 - 1/(1 + (w_1/K_2)^{n_2})k_2X_2$$

which depict two subpopulations (X_1 and X_2) with proliferation rate constants r_1 and r_2 respectively, and basal interconversion rate constants (r_1 and r_2 for X_1-to-X_2 conversion and X_2-to-X_1 conversion, respectively) (Figure 4A). The signal that originates from X_1 and received by X_2 is modeled by an inhibitory Hill function that influences the overall conversion rate from X_2 to X_1, as the inferred inter- and intra-cellular activities common to all cancer types. Parameter K_2 determines the threshold of the inactivation and n_2 determines the nonlinearity of the response. w_1 is the abundance of X_1 relative to the total size of the population (i.e. $w_1 = X_1/(X_1 + X_2)$. This Hill function effectively serves as a feedback mechanism that may influence the dynamics of the cancer cell population. Simply, the model describes the dynamics of a cell population with two discrete states (of any type) with interactions between them.

We simulated the model with an initial population containing X_1 but not X_2 with a parameter set adjusted such that the steady state ratio of the two populations is approximately 1:1 (Figure 4B, red), a ratio consistent with experimentally observed NE to non-NE transitions of SCLC cells[15]. We found that removing the feedback resulted in a lower steady state fraction of X_2 due to the increased number of cells converting from X_2 to X_1 (Figure 4B, black). While this might suggest a role of the feedback signaling (Figure 4A, red) in facilitating the formation of mesenchymal-like X_2 cell population, one can argue that this performance advantage can be simply achieved by adjusting the basal conversion rate constant k_2. We therefore tested another feedback-free model in which there was a compensatory reduction of k_2 (Figure 4B, blue) that produced the same 1:1 steady state ratio for the two types of cells. We found that the model with the inter-subtype signaling needed a significantly shorter time to achieve the equilibrium of the two subpopulations compared to the perturbed model that achieved the same level of heterogeneity. We found that this acceleration was consistent in a range of steady state (target) ratios of the two subpopulations, but it was more prominent when the two subpopulations were comparable in size (Figure 4C). We expect that this acceleration function may help the tumor cell population to re-establish a heterogeneous population under a subtype-specific “fractional condition,” i.e., a depletion of one of the subtypes. Indeed, after we perturbed a population already at equilibrium with equal numbers of each state (X_1:X_2 ratio of 1:1) by removing 90% of X_2 cells from the system, the model with feedback recovered more rapidly compared to the feedback-free model (Figure

4D). Taken together, our mathematical model suggests a role of inter-subtype communication—inferred from single-cell data—in accelerating the acquisition of heterogeneous tumor cell population from either a relatively homogeneous initial or out-of-equilibrium population.

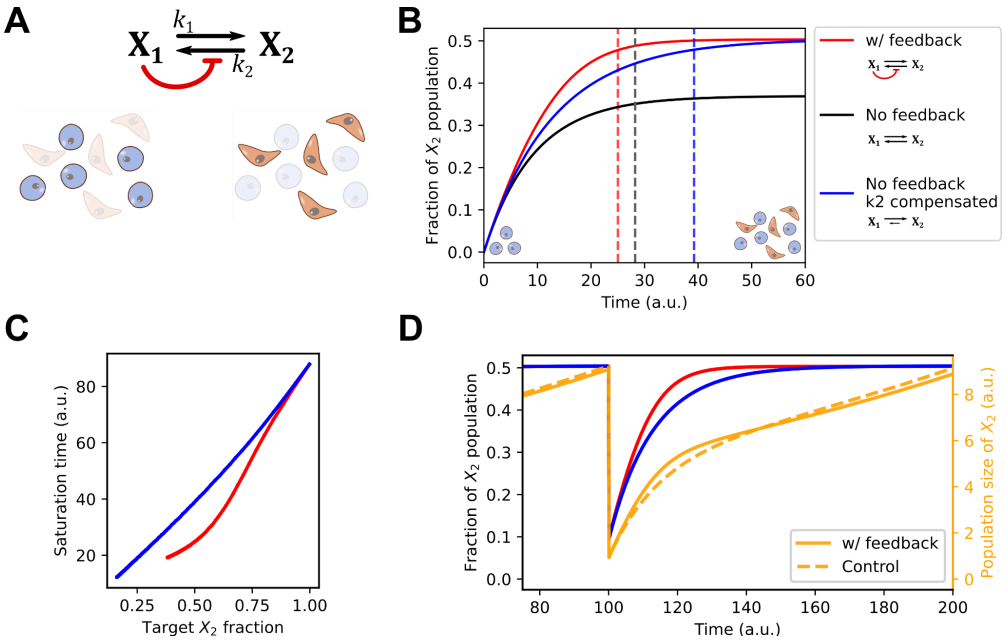

Figure 4: ***A mathematical model for inter-subtype communication.*** A) Network diagram and illustration of two cell types (Epithelial-like and Mesenchymal-like). X_1 and X_2 are two state variables representing the sizes of the two cell populations, respectively. Black arrows show transitions. Red arrow shows the intercellular communication responsible for maintaining the M-like cell state. B) Time course trajectories (solid curves) for the main model and two perturbed models. Y-axis shows the quantity $X_2/(X_1+X_2)$. Dashed vertical lines show the positions of saturation times, defined as the time at which 95% of the steady state level of the fraction is reached. C) Saturation time as a function of steady state fraction of X_2. Color code is the same as Panel B. Basal k_2 values were varied to achieve various steady state X_2 fractions. D) Time course trajectories of a fractional killing scenario in which the fractions of the two populations reached steady state and 90% of X_2 cells were removed at Time 100. The orange lines are the total population size and the red and blue lines represent X_2 fraction from the same models shown in *B*. The control model (blue and dashed orange lines) is the no-feedback model with compensated k_2.

Discussion

Elucidating the dynamics and mechanisms that govern phenotypic plasticity within cancer tumors is essential for developing therapeutic strategies and tackling two major unresolved clinical challenges: cancer metastasis and therapeutic resistance[10,11]. While considerable progress has been made in characterizing phenotypic plasticity at the gene expression level[12,60–62], many aspects remain poorly understood. Identifying the mechanisms that drive intratumoral heterogeneity and regulate phenotypic plasticity is a critical step for effective cancer treatment, as different cell types within a tumor can respond differently to therapies[22,63–67]. In this study, we investigated whether intercellular communications play a role in controlling cell fate transitions and whether these interactions stabilize or destabilize cellular phenotypes. We applied a multiscale

inference-based approach to different solid tumor scRNA-seq datasets to investigate the crosstalk between cell states and how they influence one another. Within SCLC, we found the pivotal role of intercellular signaling in maintaining the phenotypic diversity among the cancer cell population, particularly in the context of EMT. The inferred P/Y signaling network captures the activation of *Myc and* Notch signaling, which is consistent with recent observations as the activation of these two components is seen within the non-NE subtypes[16,21]. Additionally, the networks capture the mesenchymal nature of P/Y subtype[24], as the activation of many differentially overexpressed mesenchymal markers are present within the network. Furthermore, this mesenchymal phenotype is influenced by both mesenchymal P/Y cells and the more epithelial A2 cells through the activation of EMT pathways Notch and Jam. The A2 network displays similar patterns in that it utilizes both paracrine and autocrine EMT signals to maintain its epithelial state. Among several cancer types that we analyzed, this epithelial state maintenance mechanism appears to be unique to SCLC and specific to the A2 subtype.

Applying this multiscale methodology to the colon and HER2 cancer datasets yielded less-comprehensive networks. One possible explanation for this difference is that the tumor microenvironment (apart from tumor cell heterogeneity) may play a larger role in influencing phenotypic plasticity in colon and HER2 breast cancer. In all three datasets, we only examined the intercellular communications within the cancerous population. In SCLC, the cell–cell communication between the cancerous cells appears sufficient enough to influence the cellular phenotypes. However, this does not appear to be the case with colon and HER2 cancers, where other factors in the tumor microenvironment may have a greater impact on tumor cell plasticity[68,69]. The HER2 data was derived from an *in vivo* setting and this context introduces greater complexity, as interactions with surrounding non-cancerous cells could significantly shape the phenotypic diversity observed. Alternatively, technical differences in how tumor cells are classified could affect differences in inferred networks. Our method requires sufficient cellular diversity (i.e. number of cells for each cell state or significant differences in gene expression between cell states) within the dataset in order to make inferences. The cancer cells in SCLC have been categorized via archetype analysis, which identifies the most relevant features to distinguish the cell classes in high-dimensional feature space. The cells in the colon cancer dataset were FACs sorted based on EpCam expression and they were assigned epithelial and mesenchymal scores through gene set enrichment analysis. The HER2 cell identities were inferred using single-cell trajectory analysis in which the terminal branches were used to annotate cells based on the differential expression of known marker genes. These differences in classification methods could influence the resolution of cell states and the inferred diversity within the datasets, potentially limiting the ability to detect nuanced intercellular communication networks in colon and HER2.

Phenotypic diversity in cell populations can be supported by both autonomous and non-autonomous mechanisms. Autonomous mechanisms include intrinsic transcriptional fluctuations, which can stochastically initiate phenotypic transitions[61], as well as multi-stable regulatory networks, where cells can switch between stable

phenotypic states based on underlying network architectures[70]. Additionally, post-transcriptional mechanisms provide another layer of intrinsic regulation[71]. However, while these autonomous processes can trigger phenotypic transition, it may be difficult to maintain this phenotypic diversity over time. Therefore, non-autonomous mechanisms may be required, such as paracrine/autocrine signaling which can play a critical role in reinforcing phenotypic heterogeneity through intercellular communication[58,72,73]. Our findings highlight the importance of these non-autonomous signaling mechanisms, demonstrating that cell–cell interactions can be essential for sustaining the intratumoral phenotypic heterogeneity.

Cell–cell interactions are fundamental to shaping and maintaining multicellular structures and tissue integrity. Among these, cell–cell communications play a pivotal role in coordinating cellular behavior across short and long distances within tissues. Here, we inferred cell–cell communications from scRNA-seq data, and while cell–cell communication methods based on scRNA-seq can predict short-range communications[69,74], they are limited by the lack of spatial context and can introduce significant false-positives[75]. Integrating spatial transcriptomics with scRNA-seq offers a promising avenue to overcome these limitations, as it preserves the spatial arrangement of cells, allowing for more accurate inference of both short- and long-range communications[76,77]. Future work will benefit from leveraging these integrative approaches as it will refine our understanding of the role of cell–cell communications in maintaining intratumoral heterogeneity within tumors.

Intercellular signaling is known to contribute to the intratumoral heterogeneity within SCLC, with the activation of Notch signaling resulting in NE to non-NE cell fate switching in 10–50% of tumor cells[15]. Additionally, the non-NE subtype exhibits a reduced proliferative rate but relatively greater chemoresistance, and these cells support the growth and survival of the NE subtype within admixed tumors[18]. This dynamic interplay between NE and non-NE subtypes highlights the role of intercellular signaling in maintaining a functional heterogeneity that benefits tumor survival and progression. A recent study suggests that SCLC subtypes not only coexist but may actively cooperate to optimize essential tumor functions, with NE and non-NE cells interacting in mutually beneficial ways to foster tumor growth and adapt to changing external conditions, such as treatment[21]. Additionally, it has been suggested that non-genetic mechanisms, such as cell-cell interactions between SCLC cell types, provides the capability for some tumors to reemerge once therapy is withdrawn through commensal niche-like interactions, where one cell type fosters the growth or survival of another[22]. These cooperative interactions are critical for maintaining the phenotypic diversity needed for tumor adaptability. Importantly, the rate at which phenotypic heterogeneity reaches equilibrium is likely driven by such cooperative mechanisms, enabling tumors to rapidly adapt by leveraging the distinct but complementary functions of different cell types. Disrupting these signaling networks or undermining the cooperative interactions between subtypes could impair the tumor’s ability to maintain this adaptability. thereby enhancing therapeutic efficacy.

We are only beginning to uncover the role in cancer of non-cell-autonomous signaling on phenotypic plasticity—a key driver of tumor progression and therapeutic resistance. Our results indicate that SCLC tumor cells have significant responses to extracellular signals emanating from different tumor cell subtypes and that transitions to mesenchymal phenotypes (especially P/Y) are enhanced by ligands released from both NE and nonNE sources. Additionally, and somewhat surprisingly, the more epithelial A2 state is likewise stabilized by signals from both NE and nonNE sources. Our mathematical model of the dynamics of cell state heterogeneity equilibration suggests that feedback mechanisms dependent on intercellular signaling are important modulators of how quickly equilibrium can be reestablished. Altogether, our results support an important role for intercellular communication in controlling the dynamics of establishing equilibrium of intrinsic tumor cell state heterogeneity.

Methods

Single-cell RNA-Sequencing Data

Single-cell RNA sequencing data were downloaded from Gene Expression Omnibus (GEO) at GSE149180 (RPM mouse tumor time course)[16], GSE138474 (Human SCLC CDX)[25], GSE154930 (HCT116 colon cancer)[33], and GSE152422 (HER2 breast cancer mouse isoform). RPM mouse tumor dataset was preprocessed as described by Groves et al.[21] Python package *Scanpy* (version 1.8.0) was used for filtering and normalization of total counts. Log-transformation was performed using the *log1p* function from the *Numpy* (version 1.17) package and scaling was done using *Scanpy*.

Human CDX data were preprocessed as described by Gay et al.[78] Cells were filtered to remove non-tumor cells. Only the SC53 tumors were used in this analysis. *Scanpy* was used to normalize the total counts by cell and the data was then log-transformed.

Cell type annotation for RPM and SC53 datasets was performed as described by Groves, et al.[21] Briefly, archetypal analysis was applied to gene expression data. This approximates the cell phenotype space as a low dimensional polytope that encapsulates the gene expression data. The vertices of this multi-dimensional space represent archetypes, each optimal for a specific functional task. In the RPM dataset, there are some cell type labels that consist of 2 transcriptional states (A/N and P/Y). This is due to these cells falling in between these two archetypes.

The deposited colon cancer data was already preprocessed as described by Sacchetti, et al.[33] $EpCAM^{high}$ and $EpCAM^{low}$ raw count matrices were merged together in R and processed for downstream analysis using the *Seurat* package. Dimension

reduction was performed using PCA, tSNE, and UMAP. Cell type annotation was performed based on EpCAM expression. Cells were also assigned epithelial and mesenchymal scores which were computed using gene set enrichment scoring packages.

HER2 breast cancer data was preprocessed as described by Ginzel, et al.[34] Raw count matrices were processed using *Seurat* (version 4.0.0). Scores for S-phase and G_2-M cell-cycle using the *CellCycleScoring* function. Data were log-normalized and scaled after regressing out total UMI counts, percent mitochondrial gene expression, and cell-cycle phase. Dimension reduction was done using PCA and UMAP. Individual clusters were annotated based on known marker gene expression. Trajectory analysis was performed with *Monocle 2* (version 2.12.0) on a subset of the data which contains only the epithelial compartment, and cellular identities were inferred in the terminal branches using gene set enrichment analysis.

Cell-Cell Communication Inference

The *CellChat* (version 1.6.1) package in R was used to infer intercellular communications. *CellChat* can quantitatively infer and analyze intercellular communication networks from scRNA-seq data. The interactions were identified and quantified based on the differentially over-expressed ligands and receptors for each cell group and a mass action-based model is used to integrate all known molecular interactions, including the core interaction between ligands and receptors with multi-subunit structure, as well as any additional modulation by cofactors.

Differential Expression Analysis and Transcription Factor Activity Inference

Differential expression analysis was performed using *Seurat's FindMarkers* function. The function was applied to each cell type within the dataset. The differential expression results were then filtered for significance ($p < 0.05$). The statistically significant differentially expressed genes were then used for downstream processes.

Transcription factor activity inference was performed using *decoupleR*'s (version 2.6.0) univariate linear model method. This method requires gene expression values and a gene regulatory network as inputs. *decoupleR* provides the *CollecTRI* network which comprises a curated collection of signed TF-target gene interactions, weighted based on the mode of regulation[79]. This method will fit a linear model for each cell and each TF in the network, predicting the observed gene expression based on the TF-target gene interaction weights[80]. The average log fold-change values were used for

the expression data input and the CollecTRI gene regulatory network was utilized for the network input. This was done for each cell type, so the differential expression results used in the function were specific to that cell type. Once the model is fitted, the obtained t-value of the slope is the score. The list of inferred active TFs was filtered for significance ($p < 0.05$) and activity (score > 0). The resulting inferred active TFs serve as inputs for the next step in the pipeline.

Signaling Network Inference

The LIANA+ framework (version 1.0.2) was utilized to infer the signaling network. The *find_causalnet* function utilizes the *CARNIVAL* algorithm in the *CORNETO* package (v0.9.1-a5) to infer the signaling network from receptors to transcription factors. *CARNIVAL* integrates prior knowledge of signed and directed protein-protein interactions from *OmniPath*[81] to construct the smallest-sign consistent network that explains the measured inputs and outputs.

CARNIVAL requires a prior knowledge graph, receptor input scores, TF output scores, and node weights. This incorporation ensures the resulting network captures both dataset-specific information and established biological knowledge. For the receptor input scores, we utilized the probability score inferred from *CellChat*. Given that some receptors were inferred to be involved in multiple ligand-receptor interactions, we added the probability scores for a receptor if the inferred signaling pathway was the same. All inferred receptors were used as inputs for the signaling network algorithm. For the TF output scores, we used only the inferred active transcription factors.

The prior knowledge graph was created using the LIANA+ function, *build_prior_network.* Intracellular signaling Interactions were obtained from OmniPath using the *OmnipathR* (version 3.8.2) package. Interactions were obtained from the *omnipath, kinaseextra,* and *pathwayextra* datasets. The datasets were filtered based on curation effort (curation_effort > 1). The prior knowledge graph was created using the filtered interactions, input receptors, and output transcription factors. The nodes within the graph were assigned weights based on cell-type specific differential expression. Node weights had to be scaled from zero to one so the *MinMaxScaler* function from the Python library, *scikit-learn* (version 1.3.1), was used to scale the average log2 fold-change values.

The *CVXPY* (version 1.3.2) backend and *GUROBI* optimizer (*gurobipy* version 10.0.3) were used within the signaling network algorithm.

The *CARNIVAL* algorithm will return the smallest sign-consistent network from the input receptors to the output TFs. In the resultant network, ligands are reincorporated based on the L-R interactions from *CellChat*, while downstream target genes were added to the network based on the consistency of mode of regulation from upstream TF and differential expression of target gene. For example, an activating edge towards a target gene necessitates a positive log fold-change value within the target gene in order for the gene to be added to the network. We used cell state-specific differential expression results for each network. TF-regulon interactions were obtained using *OmnipathR* via the *import_transcriptional_interactions* function. The interactions were filtered so that only SCLC[21] (only for RPM and SC53 dataset) and EMT[82] marker target genes were contained within the interaction list. Additionally, the list was filtered to contain experimentally validated interactions (curation_effort > 0).

The code of our new multiscale inference pipeline is available at https://github.com/DanielL543/scRNA_seq_multiscale_inference.

Statistical Analysis of Networks

The cell-type specific differential expression results were used to determine the proportion of differentially expressed genes being in network vs out of network and whether the gene is lineage supporting or not. Lineage supporting genes were determined based on the previously reported phenotype of the cell type. Fisher's exact test was then performed to determine the significance of a differentially expressed being in network and being lineage supporting.

Mathematical Modeling

The ODE system shown in Eq 1 was used to simulate a cell population containing two subtypes of cancer cells. A representative parameter set was used for simulations: $r_1 = 0.01$, $r_2 = 0.001$, $k_1 = k_2 = 0.04$, $K_2 = 0.5$, and $n_2 = 6$. For feedback-free models (control), K_2 was set to 1000. k_2 was adjusted to allow a feedback-free model (k_2 compensated model) to achieve desired fraction of X_2 cells. The model is dimensionless.

Acknowledgements

This work is supported by grants from National Institutes of Health (R35GM149531) and from National Science Foundation (2243562) awarded to T.H.

References

1. Vitale, I., Shema, E., Loi, S. & Galluzzi, L. Intratumoral heterogeneity in cancer progression and response to immunotherapy. *Nat Med* **27**, 212–224 (2021).
2. Burkhardt, D. B., San Juan, B. P., Lock, J. G., Krishnaswamy, S. & Chaffer, C. L. Mapping Phenotypic Plasticity upon the Cancer Cell State Landscape Using Manifold Learning. *Cancer Discov* **12**, 1847–1859 (2022).
3. Hanahan, D. Hallmarks of Cancer: New Dimensions. *Cancer Discov* **12**, 31–46 (2022).
4. Marine, J.-C., Dawson, S.-J. & Dawson, M. A. Non-genetic mechanisms of therapeutic resistance in cancer. *Nat Rev Cancer* **20**, 743–756 (2020).
5. Marusyk, A., Janiszewska, M. & Polyak, K. Intratumor heterogeneity: the Rosetta stone of therapy resistance. *Cancer Cell* **37**, 471–484 (2020).
6. McGranahan, N. & Swanton, C. Clonal Heterogeneity and Tumor Evolution: Past, Present, and the Future. *Cell* **168**, 613–628 (2017).
7. Sun, X. & Yu, Q. Intra-tumor heterogeneity of cancer cells and its implications for cancer treatment. *Acta Pharmacol Sin* **36**, 1219–1227 (2015).
8. Flavahan, W. A., Gaskell, E. & Bernstein, B. E. Epigenetic plasticity and the hallmarks of cancer. *Science* **357**, eaal2380 (2017).
9. Welch, D. R. & Hurst, D. R. Defining the Hallmarks of Metastasis. *Cancer Research* **79**, 3011–3027 (2019).
10. Gupta, P. B., Pastushenko, I., Skibinski, A., Blanpain, C. & Kuperwasser, C. Phenotypic Plasticity: Driver of Cancer Initiation, Progression, and Therapy Resistance. *Cell Stem Cell* **24**, 65–78 (2019).

11. Jain, P. *et al.* Dynamical hallmarks of cancer: Phenotypic switching in melanoma and epithelial-mesenchymal plasticity. *Semin Cancer Biol* **96**, 48–63 (2023).
12. Pillai, M. & Jolly, M. K. Systems-level network modeling deciphers the master regulators of phenotypic plasticity and heterogeneity in melanoma. *iScience* **24**, (2021).
13. Stylianou, N. *et al.* A molecular portrait of epithelial–mesenchymal plasticity in prostate cancer associated with clinical outcome. *Oncogene* **38**, 913–934 (2019).
14. Watanabe, K., Panchy, N., Noguchi, S., Suzuki, H. & Hong, T. Combinatorial perturbation analysis reveals divergent regulations of mesenchymal genes during epithelial-to-mesenchymal transition. *npj Syst Biol Appl* **5**, 1–15 (2019).
15. Lim, J. S. *et al.* Intratumoural heterogeneity generated by Notch signalling promotes small-cell lung cancer. *Nature* **545**, 360–364 (2017).
16. Ireland, A. S. *et al.* MYC Drives Temporal Evolution of Small Cell Lung Cancer Subtypes by Reprogramming Neuroendocrine Fate. *Cancer Cell* **38**, 60-78.e12 (2020).
17. Gazdar, A. F., Bunn, P. A. & Minna, J. D. Small-cell lung cancer: what we know, what we need to know and the path forward. *Nat Rev Cancer* **17**, 725–737 (2017).
18. Calbo, J. *et al.* A functional role for tumor cell heterogeneity in a mouse model of small cell lung cancer. *Cancer Cell* **19**, 244–256 (2011).
19. Shue, Y. T. *et al.* A conserved YAP/Notch/REST network controls the neuroendocrine cell fate in the lungs. *Nat Commun* **13**, 2690 (2022).
20. Wooten, D. J. *et al.* Systems-level network modeling of Small Cell Lung Cancer subtypes identifies master regulators and destabilizers. *PLoS Comput Biol* **15**,

e1007343 (2019).

21. Groves, S. M. *et al.* Archetype tasks link intratumoral heterogeneity to plasticity and cancer hallmarks in small cell lung cancer. *Cell Syst* **13**, 690-710.e17 (2022).
22. Gopal, P. *et al.* Multivalent state transitions shape the intratumoral composition of small cell lung carcinoma. *Science Advances* **8**, eabp8674 (2022).
23. Rudin, C. M. *et al.* Molecular subtypes of small cell lung cancer: a synthesis of human and mouse model data. *Nat Rev Cancer* **19**, 289–297 (2019).
24. Groves, S. M. *et al.* Involvement of Epithelial-Mesenchymal Transition Genes in Small Cell Lung Cancer Phenotypic Plasticity. *Cancers (Basel)* **15**, 1477 (2023).
25. Stewart, C. A. *et al.* Single-cell analyses reveal increased intratumoral heterogeneity after the onset of therapy resistance in small-cell lung cancer. *Nat Cancer* **1**, 423–436 (2020).
26. Allison Stewart, C. *et al.* Dynamic variations in epithelial-to-mesenchymal transition (EMT), ATM, and SLFN11 govern response to PARP inhibitors and cisplatin in small cell lung cancer. *Oncotarget* **8**, 28575–28587 (2017).
27. Dongre, A. & Weinberg, R. A. New insights into the mechanisms of epithelial–mesenchymal transition and implications for cancer. *Nat Rev Mol Cell Biol* **20**, 69–84 (2019).
28. Mollaoglu, G. *et al.* MYC Drives Progression of Small Cell Lung Cancer to a Variant Neuroendocrine Subtype with Vulnerability to Aurora Kinase Inhibition. *Cancer Cell* **31**, 270–285 (2017).
29. Dimitrov, D. *et al.* LIANA+: an all-in-one cell-cell communication framework. Preprint

at https://doi.org/10.1101/2023.08.19.553863 (2023).

30. Jin, S. *et al.* Inference and analysis of cell-cell communication using CellChat. *Nat Commun* **12**, 1088 (2021).
31. Dimitrov, D. *et al.* Comparison of methods and resources for cell-cell communication inference from single-cell RNA-Seq data. *Nat Commun* **13**, 3224 (2022).
32. Liu, A. *et al.* From expression footprints to causal pathways: contextualizing large signaling networks with CARNIVAL. *npj Syst Biol Appl* **5**, 1–10 (2019).
33. Sacchetti, A. *et al.* Phenotypic plasticity underlies local invasion and distant metastasis in colon cancer. *Elife* **10**, e61461 (2021).
34. Ginzel, J. D. *et al.* HER2 Isoforms Uniquely Program Intratumor Heterogeneity and Predetermine Breast Cancer Trajectories During the Occult Tumorigenic Phase. *Mol Cancer Res* **19**, 1699–1711 (2021).
35. Zhang, H. *et al.* AGRN promotes lung adenocarcinoma progression by activating Notch signaling pathway and acts as a therapeutic target. *Pharmacol Res* **194**, 106819 (2023).
36. Gjerdrum, C. *et al.* Axl is an essential epithelial-to-mesenchymal transition-induced regulator of breast cancer metastasis and patient survival. *Proceedings of the National Academy of Sciences* **107**, 1124–1129 (2010).
37. Gordon, K. J., Kirkbride, K. C., How, T. & Blobe, G. C. Bone morphogenetic proteins induce pancreatic cancer cell invasiveness through a Smad1-dependent mechanism that involves matrix metalloproteinase-2. *Carcinogenesis* **30**, 238–248 (2009).
38. Pickup, M. W. *et al.* Deletion of the BMP receptor BMPR1a impairs mammary tumor

formation and metastasis. *Oncotarget* **6**, 22890–22904 (2015).

39. Lu, Z., Ghosh, S., Wang, Z. & Hunter, T. Downregulation of caveolin-1 function by EGF leads to the loss of E-cadherin, increased transcriptional activity of. *CANCER CELL* (2003).
40. Shibue, T. & Weinberg, R. A. EMT, CSCs, and drug resistance: the mechanistic link and clinical implications. *Nat Rev Clin Oncol* **14**, 611–629 (2017).
41. Lo, H.-W. *et al.* Epidermal Growth Factor Receptor Cooperates with Signal Transducer and Activator of Transcription 3 to Induce Epithelial-Mesenchymal Transition in Cancer Cells via Up-regulation of TWIST Gene Expression. *Cancer Research* **67**, 9066–9076 (2007).
42. Pirozzi, G. *et al.* Epithelial to Mesenchymal Transition by TGFβ-1 Induction Increases Stemness Characteristics in Primary Non Small Cell Lung Cancer Cell Line. *PLOS ONE* **6**, e21548 (2011).
43. Tomlinson, D. C., Baxter, E. W., Loadman, P. M., Hull, M. A. & Knowles, M. A. FGFR1-Induced Epithelial to Mesenchymal Transition through MAPK/PLCγ/COX-2-Mediated Mechanisms. *PLOS ONE* **7**, e38972 (2012).
44. Tian, Y. *et al.* Junctional adhesion molecule-A, an epithelial–mesenchymal transition inducer, correlates with metastasis and poor prognosis in human nasopharyngeal cancer. *Carcinogenesis* **36**, 41–48 (2015).
45. Communal, L. *et al.* Low junctional adhesion molecule-A expression is associated with an epithelial to mesenchymal transition and poorer outcomes in high-grade serous carcinoma of uterine adnexa. *Modern Pathology* **33**, 2361–2377 (2020).

46. Lamouille, S., Xu, J. & Derynck, R. Molecular mechanisms of epithelial-mesenchymal transition. *Nat Rev Mol Cell Biol* **15**, 178–196 (2014).
47. Abedini, A., Sayed, C., Carter, L. E., Boerboom, D. & Vanderhyden, B. C. Non-canonical WNT5a regulates Epithelial-to-Mesenchymal Transition in the mouse ovarian surface epithelium. *Sci Rep* **10**, 9695 (2020).
48. Yuan, X. *et al.* Notch signaling and EMT in non-small cell lung cancer: biological significance and therapeutic application. *Journal of Hematology & Oncology* **7**, 87 (2014).
49. Yin, J., Guo, Y. & Li, Z. Platelet-derived growth factor-B signalling might promote epithelial-mesenchymal transition in gastric carcinoma cells through activation of the MAPK/ERK pathway. *Contemporary Oncology* **25**, 1 (2021).
50. Craene, B. D. & Berx, G. Regulatory networks defining EMT during cancer initiation and progression. *Nat Rev Cancer* **13**, 97–110 (2013).
51. Xu, C. *et al.* SPP1, analyzed by bioinformatics methods, promotes the metastasis in colorectal cancer by activating EMT pathway. *Biomedicine & Pharmacotherapy* **91**, 1167–1177 (2017).
52. Nagaharu, K. *et al.* Tenascin C Induces Epithelial-Mesenchymal Transition–Like Change Accompanied by SRC Activation and Focal Adhesion Kinase Phosphorylation in Human Breast Cancer Cells. *The American Journal of Pathology* **178**, 754–763 (2011).
53. Lin, L.-C., Hsu, S.-L., Wu, C.-L. & Hsueh, C.-M. TGFβ can stimulate the p38/β-catenin/PPARγ signaling pathway to promote the EMT, invasion and migration of non-small cell lung cancer (H460 cells). *Clin Exp Metastasis* **31**, 881–895 (2014).

54. Kalluri, R. & Weinberg, R. A. The basics of epithelial-mesenchymal transition. *J Clin Invest* **119**, 1420–1428 (2009).

55. Qi, L. *et al.* Wnt3a expression is associated with epithelial-mesenchymal transition and promotes colon cancer progression. *Journal of Experimental & Clinical Cancer Research* **33**, 107 (2014).

56. Yang, D. *et al.* WNT4 secreted by tumor tissues promotes tumor progression in colorectal cancer by activation of the Wnt/β-catenin signalling pathway. *Journal of Experimental & Clinical Cancer Research* **39**, 251 (2020).

57. Mandicourt, G., Iden, S., Ebnet, K., Aurrand-Lions, M. & Imhof, B. A. JAM-C Regulates Tight Junctions and Integrin-mediated Cell Adhesion and Migration *. *Journal of Biological Chemistry* **282**, 1830–1837 (2007).

58. Gregory, P. A. *et al.* An autocrine TGF-beta/ZEB/miR-200 signaling network regulates establishment and maintenance of epithelial-mesenchymal transition. *Mol Biol Cell* **22**, 1686–1698 (2011).

59. Scheel, C. *et al.* Paracrine and autocrine signals induce and maintain mesenchymal and stem cell states in the breast. *Cell* **145**, 926–940 (2011).

60. Torre, E. A. *et al.* Genetic screening for single-cell variability modulators driving therapy resistance. *Nat Genet* **53**, 76–85 (2021).

61. Schuh, L. *et al.* Gene Networks with Transcriptional Bursting Recapitulate Rare Transient Coordinated High Expression States in Cancer. *Cell Syst* **10**, 363-378.e12 (2020).

62. Akbar, M. W. *et al.* A Stemness and EMT Based Gene Expression Signature Identifies Phenotypic Plasticity and is A Predictive but Not Prognostic Biomarker for

Breast Cancer. *J Cancer* **11**, 949–961 (2020).

63. Housman, G. *et al.* Drug Resistance in Cancer: An Overview. *Cancers* **6**, 1769–1792 (2014).
64. Nami, B., Ghanaeian, A., Black, C. & Wang, Z. Epigenetic Silencing of HER2 Expression during Epithelial-Mesenchymal Transition Leads to Trastuzumab Resistance in Breast Cancer. *Life* **11**, 868 (2021).
65. Jordan, N. V. *et al.* HER2 expression identifies dynamic functional states within circulating breast cancer cells. *Nature* **537**, 102–106 (2016).
66. Kim, C. *et al.* Chemoresistance Evolution in Triple-Negative Breast Cancer Delineated by Single-Cell Sequencing. *Cell* **173**, 879-893.e13 (2018).
67. Tirosh, I. *et al.* Dissecting the multicellular ecosystem of metastatic melanoma by single-cell RNA-seq. *Science* **352**, 189–196 (2016).
68. Zapatero, M. R. *et al.* Trellis tree-based analysis reveals stromal regulation of patient-derived organoid drug responses. *Cell* **186**, 5606-5619.e24 (2023).
69. Qin, X. *et al.* An oncogenic phenoscape of colonic stem cell polarization. *Cell* **186**, 5554-5568.e18 (2023).
70. Ye, Y., Kang, X., Bailey, J., Li, C. & Hong, T. An enriched network motif family regulates multistep cell fate transitions with restricted reversibility. *PLOS Computational Biology* **15**, e1006855 (2019).
71. Nordick, B., Yu, P. Y., Liao, G. & Hong, T. Nonmodular oscillator and switch based on RNA decay drive regeneration of multimodal gene expression. *Nucleic Acids Research* **50**, 3693–3708 (2022).

72. Neelakantan, D. *et al.* EMT cells increase breast cancer metastasis via paracrine GLI activation in neighbouring tumour cells. *Nat Commun* **8**, 15773 (2017).

73. Yamamoto, M. *et al.* NF-κB non-cell-autonomously regulates cancer stem cell populations in the basal-like breast cancer subtype. *Nat Commun* **4**, 2299 (2013).

74. Choi, H. *et al.* Transcriptome Analysis of Individual Stromal Cell Populations Identifies Stroma-Tumor Crosstalk in Mouse Lung Cancer Model. *Cell Reports* **10**, 1187–1201 (2015).

75. Almet, A. A., Cang, Z., Jin, S. & Nie, Q. The landscape of cell–cell communication through single-cell transcriptomics. *Current Opinion in Systems Biology* **26**, 12–23 (2021).

76. Cang, Z. *et al.* Screening cell–cell communication in spatial transcriptomics via collective optimal transport. *Nat Methods* **20**, 218–228 (2023).

77. Garcia-Alonso, L. *et al.* Mapping the temporal and spatial dynamics of the human endometrium in vivo and in vitro. *Nat Genet* **53**, 1698–1711 (2021).

78. Gay, C. M. *et al.* Patterns of transcription factor programs and immune pathway activation define four major subtypes of SCLC with distinct therapeutic vulnerabilities. *Cancer Cell* **39**, 346-360.e7 (2021).

79. Müller-Dott, S. *et al.* Expanding the coverage of regulons from high-confidence prior knowledge for accurate estimation of transcription factor activities. *Nucleic Acids Research* **51**, 10934–10949 (2023).

80. Badia-i-Mompel, P. *et al.* decoupleR: ensemble of computational methods to infer biological activities from omics data. *Bioinform Adv* **2**, vbac016 (2022).

81. Türei, D. *et al.* Integrated intra- and intercellular signaling knowledge for multicellular omics analysis. *Molecular Systems Biology* **17**, e9923 (2021).

82. Panchy, N., Watanabe, K., Takahashi, M., Willems, A. & Hong, T. Comparative single-cell transcriptomes of dose and time dependent epithelial-mesenchymal spectrums. *NAR Genom Bioinform* **4**, lqac072 (2022).